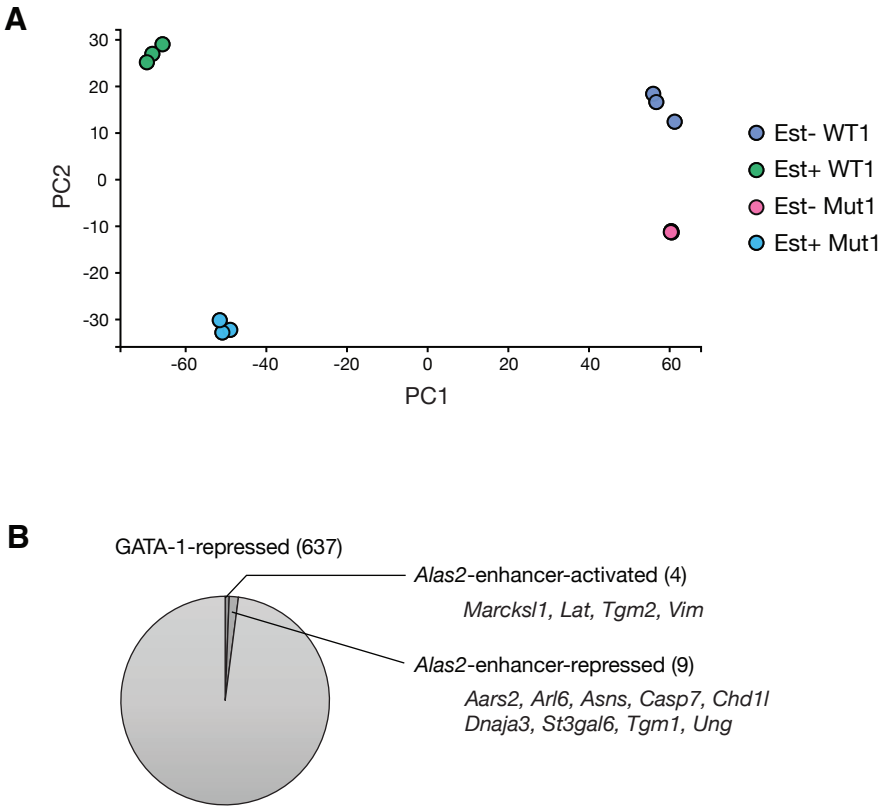

Figure S1. Principle component analysis of the proteomes and GATA-1/*Alas2*-enhancer-repressed mRNAs/proteins, Related to Figure 1.

(A) Principle component analysis of untreated and β-estradiol-treated WT and double-mutant G1E-ER-GATA-1 cell proteomes (n = 3 biological replicates).
(B) GATA-1-repressed mRNAs and proteins, also regulated by *Alas2*-enhancer, detected by RNA-seq and proteomics.

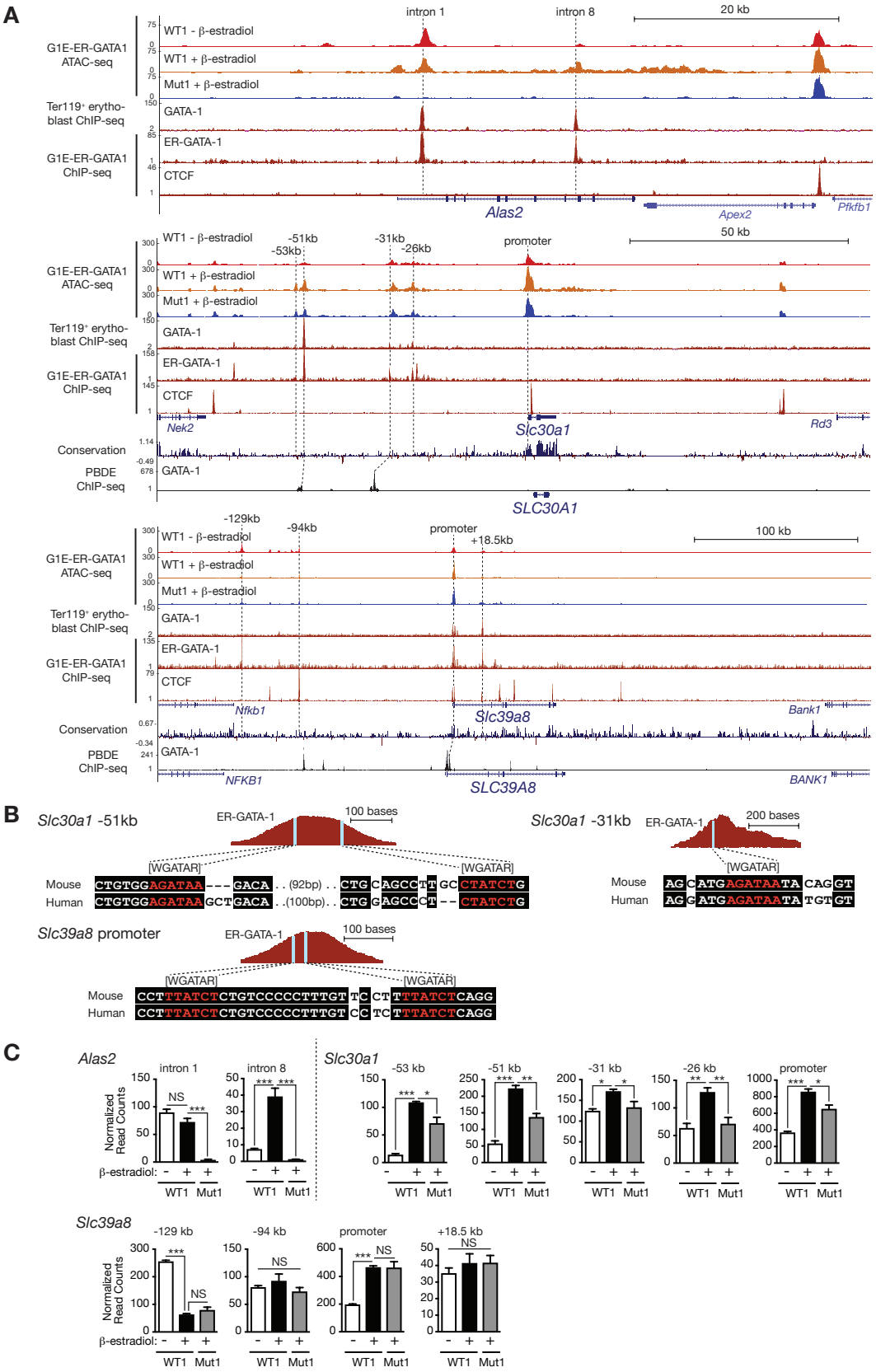

Figure S2. Mechanistic dissection of GATA-1/heme-regulated gene expression, Related to Figure 2.
(A) ATAC-seq profiles of untreated WT1 and β-estradiol-treated WT1 and *Alas2* intronic double-mutant cells and GATA-1 ChIP-seq profiles at *Alas2*, *Slc30a1*, and *Slc39a8*.
(B) Conserved GATA motifs in GATA-1 ChIP-seq peaks.
(C) Normalized ATAC-seq read counts.
P values were calculated by one-way ANOVA, followed by Dunnett's test (n = 3 biol. reps., mean +/- SE).
*P < 0.05, **P < 0.01, ***P < 0.001, NS: not significant

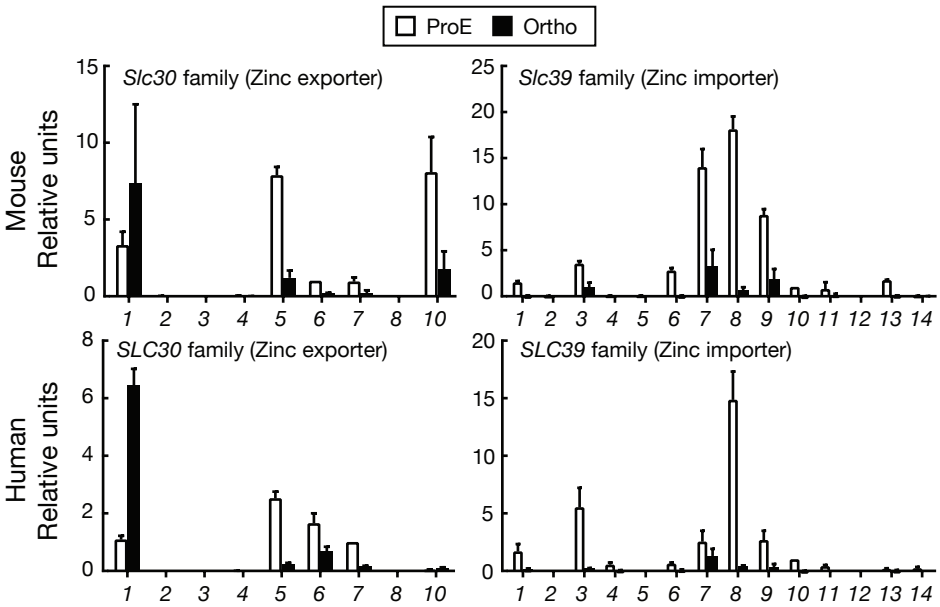

Figure S3. Expression levels of all *Slc30* (zinc exporter) and *Slc39* (zinc importer) family members in mouse and human proerythroblasts and orthochromatic erythroblasts, Related to Figure 3.

Published RNA-seq data was re-analyzed (An et al., 2014).

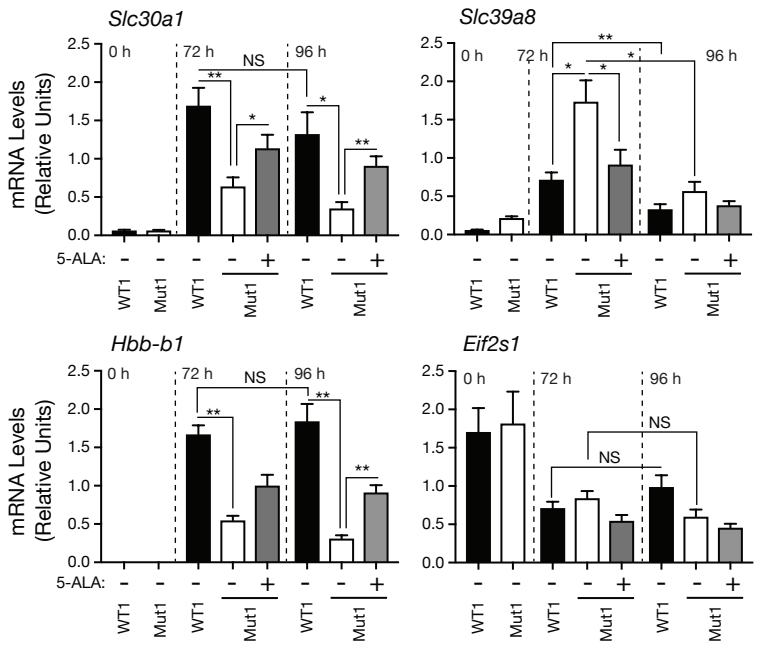

Figure S4. *Slc39a8* downregulation during erythroid maturation of wild type and *Alas2* enhancer mutant G1E-ER-GATA-1 cells, Related to Figure 3.

Real-time RT-PCR analysis of mRNA levels of *Slc30a1*, *Slc39a8*, *Hbb-b1*, and *Eif2s1* in WT and double mutant G1E-ER-GATA-1 cells (n = 6 biological replicates from three independent experiments, mean +/- SE). *P* values were calculated by repeated-measures one-way ANOVA, followed by Tukey's test. *$P < 0.05$, ** $P < 0.01$, NS: not significant.

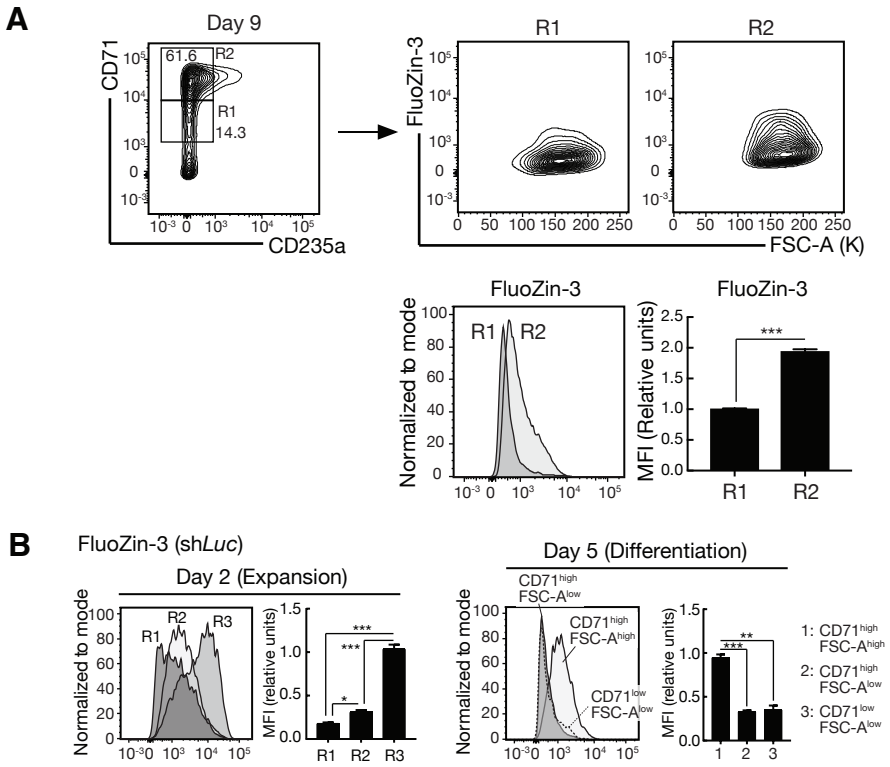

Figure S5. Increased and decreased intracellular zinc during cultured primary human and mouse erythroblast maturation, Related to Figures 4 and 6.

(A) Increased intracellular zinc during initial phases of primary human erythroblast maturation. Representative flow cytometric plots of CD71 and CD235a from differentiated human mononuclear cells from G-CSF-mobilized peripheral blood at day 9 are shown. Representative flow cytometric plots of FluoZin-3 and FSC-A and histograms of FluoZin-3 in each population are shown. FluoZin-3 MFI in each population was quantified (n = 4 biological replicates from two independent experiments, mean +/- SE). *P* values were calculated by paired two-tailed t-test. *** $P < 0.001$.
(B) Increased and decreased intracellular zinc during cultured murine erythroblast maturation. Representative histograms of FluoZin-3 in each population are shown. FluoZin-3 MFI in each population was quantified (n = 4 biological replicates from two independent experiments, mean +/- SE). *P* values were calculated by repeated-measures one-way ANOVA followed by Tukey's test. *$P < 0.05$, **$P < 0.01$; ***$P < 0.001$.

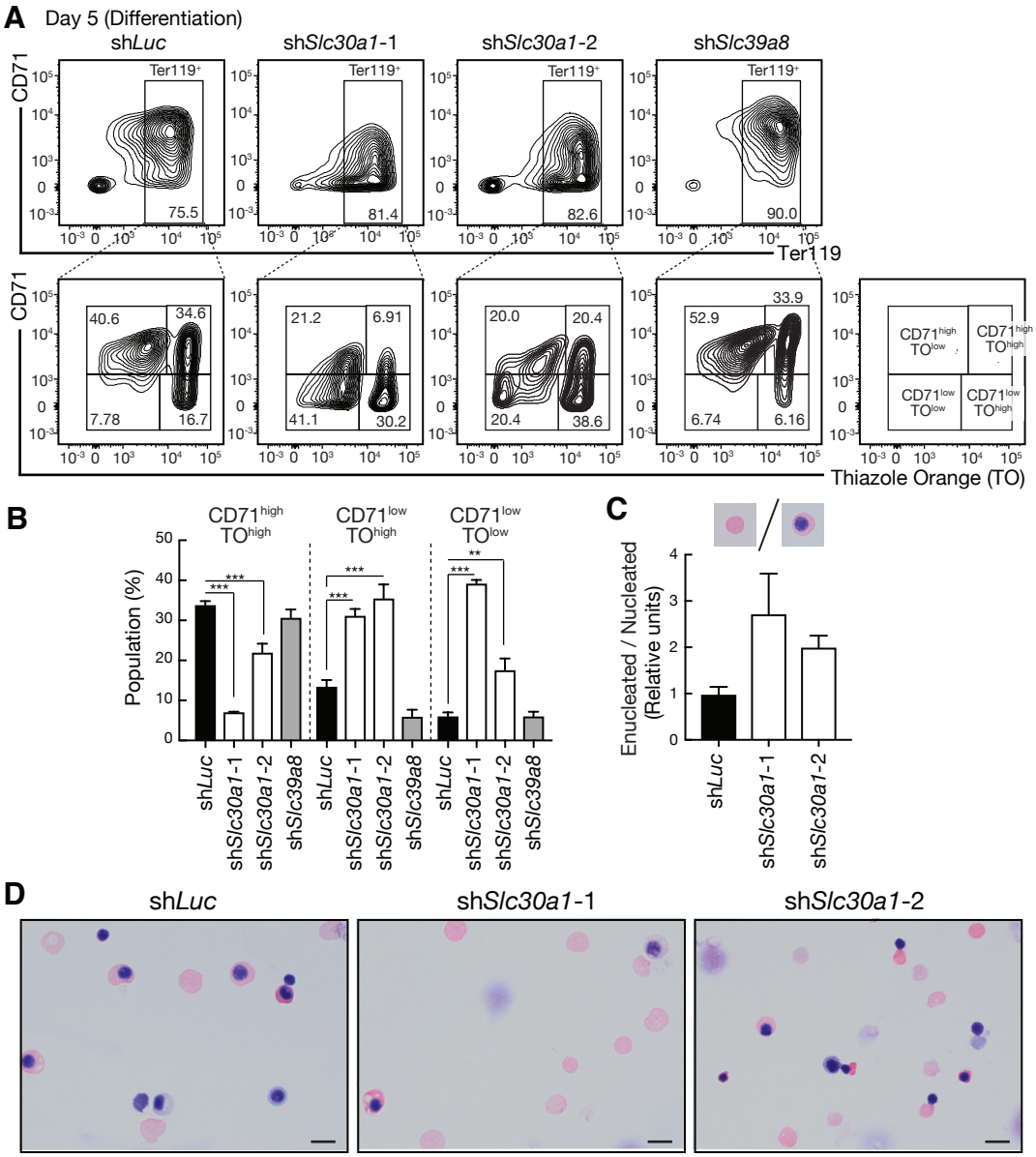

Figure S6. Intracellular zinc as a determinant of terminal differentiation, Related to Figure 6.

(A) Representative flow cytometric plots of CD71, Ter119, and thiazole orange (TO) in *Slc30a1*- or *Slc39a8*-knockdown lineage-negative hematopoietic precursors expanded for 2 days and then differentiated for 3 days.
(B) The percentage of CD71^{high}TO^{high}, CD71^{low}TO^{high}, and CD71^{low}TO^{low} populations in control and *Slc30a1*- or *Slc39a8*-knockdown cells. *P* values were calculated by one-way ANOVA, followed by Dunnett's test (n = 4 biological replicates from two independent experiments, mean +/- SE). $^{**}P < 0.01$, $^{***}P < 0.001$.
(C) The ratios of enucleated cell numbers divided by nucleated cell numbers in control and *Slc30a1*-knockdown cells (n = 2 biological replicates from one experiment, mean +/- SD).
(D) Representative photomicrographs of Wright-Giemsa staining of control and *Slc30a1*-knockdown cells. Scale bar, 10 μm.

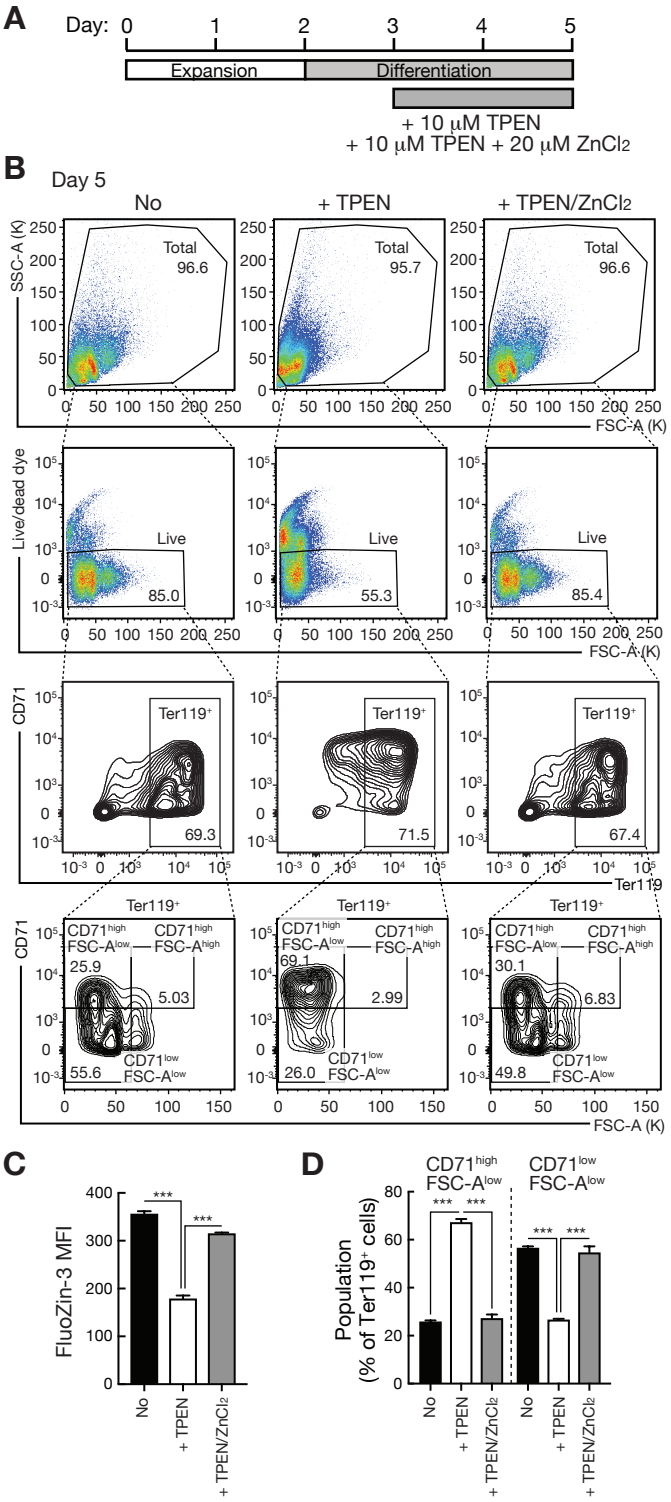

Figure S7. Reducing intracellular zinc restricts terminal differentiation, Related to Figure 6.

(A) Schematic of the experiments using the zinc chelator TPEN and $ZnCl_2$.
(B) Representative flow cytometric plots of FSC-A, SSC-A, Live/dead dye, CD71, and Ter119 at day 5.
(C) Quantitation of FluoZin-3 MFI in live populations of untreated and TPEN- or TPEN/$ZnCl_2$-treated cells. *P* values were calculated by one-way ANOVA followed by Tukey's test (n = 3 biological replicates from one experiment, mean +/- SE). *** $P < 0.001$.
(D) The percentage of $CD71^{high}FSC\text{-}A^{low}$ and $CD71^{low}FSC\text{-}A^{low}$ populations in untreated and TPEN- or TPEN/$ZnCl_2$-treated cells. *P* values were calculated by one-way ANOVA followed by Tukey's test (n = 3 biological replicates from one experiment, mean +/- SE). *** $P < 0.001$.

Table S3. Primers for qRT-PCR and oligonucleotides for construction of shRNA plasmids, Related to STAR Methods.

A

Primers for qRT-PCR	Species	Sequence (5'-> 3')
Slc30a1	mouse	caacaccagcaattccaacg tgtcagactcctggatgagattc
Slc39a8	mouse	gccagctgcacttcaacca agagaagttcgagctggttatctg
Hbb-b1	mouse	tttaacgatggcctgaatcactt cagcacaatcacgatcatattgc
18s	mouse/human	cgccgctagaggtgaaattct cgaacctccgactttcgttct
HBB	human	tcctgaggagaagtctgccgt ggagtggacagatccccaaag
HBA-1	human	gggtggacccggtcaactt gaggtgggcggccagggt
SLC30A1	human	ccaataccagcaactccaacg tacttccactgtatcaccacttctg
SLC39A8	human	gccagctgcacttcaacca gtaagactgctggacagatgacag
ACTB	human	ggccaaccgcgagaagat ccagaggcgtacagggatagc

B

shRNA	Clone ID (GE Dharmacon)	Sequence (5'-> 3') of oligonucleotide for construction of shRNA plasmid
sh*Slc30a1*-1	V2LMM_43084	tgctgttgacagtgagcgacctaagcaaatcgatatcaaatagtgaagccacagatgtatttgatatcgatttgcttagggtgcctactgcctcgga
sh*Slc30a1*-2	V3LMM_460121	tgctgttgacagtgagcgccccagtggatgtacaagtaaatagtgaagccacagatgtatttacttgtacatccactgggttgcctactgcctcgga
sh*Slc39a8*	V2LMM_72473	tgctgttgacagtgagcgccctgtcagtgacaattatcaatagtgaagccacagatgtattgataattgtcactgacaggatgcctactgcctcgga